Propane Fuel Cells Using Phosphoric-Acid-Doped Polybenzimidazole Membranes

Chin Kui Cheng, Jing Li Luo,* Karl T. Chuang, and Alan R. Sanger

Department of Chemical and Materials Engineering, University of Alberta, Edmonton, Alberta T6G 2G6, Canada

Received: December 27, 2004; In Final Form: May 4, 2005

Propane fuel cells using H_3PO_4-doped polybenzimidazole polymer membranes produce low and unsustainable current densities at temperatures up to 250 °C under anhydrous conditions. Stable intermediate species blocked the surface of noble metal anode catalysts, and the intermediate species could not react further into desorbable final products. In contrast, when water was introduced by light humidification (S_r 0.08%) of the propane stream, sustainable and higher current densities were achieved. Water participated in the reaction sequence to form surface-bound hydrocarbon and then oxygen-containing intermediates and thereby generated CO and CO_2 as the only carbon-containing products.

Background

Conventionally, the chemical energy of hydrocarbon fuels is exploited as heat through combustion to CO_2 and H_2O. Combustion of propane yields 2044.0 kJ mol^{-1} at standard temperature and pressure conditions.[1] Electrical energy can be generated by either deep or partial oxidation of hydrocarbons in a fuel cell. Hydrocarbon fuel cells offer several advantages when compared to conventional heat engines, in particular, efficient recovery of high-grade electrical energy rather than heat and better control of reaction rate and product selectivity.[2]

For fuel cell applications, hydrocarbon fuels can be reformed to H_2 and CO_2, either in a prereactor or within the anode chamber, after which the H_2 is consumed in a H_2-O_2 fuel cell.[3,4] Alternatively, the fuel can be oxidized directly to CO_2 and H_2O by reaction with oxide ions at the anode of an oxide-ion-conducting membrane electrode assembly, for example, in a solid-oxide fuel cell (SOFC).

The objective of this study is to convert propane to propylene and electrical power. To avoid deep oxidation of propane, it is necessary to use proton-conducting membranes. This type of membrane will allow the partial oxidation of propane to propylene at the anode without risk of further oxidation to CO_2.

High-Molecular-Weight Polybenzimidazole−H_3PO_4 Proton-Conducting Membranes. We have shown that membranes prepared by doping high-molecular-weight (MW) polybenzimidazole (PBI) with 500−600 mol % phosphoric acid are thermally very stable and have low gas permeability.[5] The membranes have good ionic conductivity (up to 0.032 S cm^{-1}) that was stable during operation of H_2-O_2 fuel cells over several days at temperatures up to at least 250 °C.

Conversion of Propane to Propylene. Propane can be dehydrogenated to propylene and hydrogen in a thermal equilibrium reaction (eq 1) or cracked to form elemental carbon (eq 2). Hydrogen so-generated is then available for use in H_2-O_2 fuel cells. Each of these reactions is highly endothermic. The latter reaction typically is carried out at temperatures above 800 °C and results in undesirable carbon deposits on the catalyst surface.[6]

$$C_3H_8\,(g) \rightarrow C_3H_6\,(g) + H_2\,(g) \quad (1)$$

$$C_3H_8\,(g) \rightarrow 3C + 4H_2\,(g) \quad (2)$$

However, the equilibrium concentration of hydrogen in reaction 1 is low, below 10% at temperatures up to 250 °C. Thus, to utilize reaction 1 effectively for cogeneration of propylene and electrical power in a fuel cell, hydrogen must be removed rapidly from the anode-catalyst sites as protons so as to overcome the equilibrium limitation of the reaction. Furthermore, severe conditions cannot be used, or else carbon is generated according to reaction 2, and the anode catalyst is deactivated.

In principle, it is possible to generate electricity through electrochemical oxidative dehydrogenation of propane to propylene (eqs 3−5). Water is a byproduct of the reaction (eq 4). Propane in the presence of moisture may also lead to a variety of alternative partial oxidation and deep oxidation products over anode catalysts. Herein, we will describe the use of high-MW PBI−H_3PO_4 membranes with Pt anodes and cathode catalysts in fuel cells for the conversion of propane. We will show that humidification is required for high activity and that, under these conditions, propane is converted to carbon oxides rather than propylene at temperatures up to 250 °C.

$$2C_3H_8\,(g) \rightarrow 2C_3H_6\,(g) + 4H^+ + 4e^-\ (\text{anode}) \quad (3)$$

$$4H^+ + 4e^- + O_2\,(g) \rightarrow 2H_2O\,(g)\ (\text{cathode}) \quad (4)$$

$$2C_3H_8\,(g) + O_2\,(g) \rightarrow 2C_3H_6\,(g) + 2H_2O\,(g)\ (\text{overall reaction}) \quad (5)$$

To date, no combination of anode catalyst and proton-conducting membrane has been identified for efficient cogeneration of propylene and electrical power from propane.

Hydrocarbon Fuel Cells. High-temperature hydrocarbon fuel cells are described in U.S. patents 5,747,185 and 3,718,506.[7,8] These systems operate in the temperature range 500−1200 °C

* Author to whom correspondence should be addressed. Phone: (780) 492-2232. Fax: (780) 492-2881. E-mail: jingli.luo@ualberta.ca

10.1021/jp044107a CCC: $30.25
Published on Web 06/11/2005

through generation of hydrogen using internal or external steam-reforming reactions. In contrast, Mazanec and Cable described conversion of paraffins to olefins in high-temperature solid-oxide fuel cells, thus showing the potential for cogeneration of power and propylene.[9] However, a weakness that arose from the use of oxide ion-conducting media was that the more reactive olefin products were subject to further oxidation, ultimately leading to the formation of carbon oxides and possibly reaction with byproduct water, thus limiting the efficiency and selectivity of the process.

Low-temperature hydrocarbon fuel cells normally require initial reforming of the hydrocarbon fuel into a H_2-rich gas stream, followed by purification to eliminate CO (a catalyst poison), before feeding the gas stream into the fuel cells.[10,11] There are also reports on direct utilization of hydrocarbons in electrochemical cells, in which oxidation of hydrocarbons to generate CO_2 and water was also accompanied by the formation of partial oxidation products.[12−14] These reactions were carried out in a strong acid bath, which functioned as an electrolyte and moderated the temperature of the reaction. Otsuka and Yamanaka examined applications of phosphoric acid fuel cells for partial oxidation of hydrocarbons under mild conditions (<373 K) and at 1 atm pressure, for example, for conversion of alkenes to aldehydes and organic acids, but no similar success was achieved for the conversion of alkanes.[15] When H_2-O_2 fuel cells were operated at ambient conditions and light alkanes were fed to the cathode side, there was some partial oxidation of alkanes. A limiting factor for operation of all liquid-acid fuel cells is the very low solubility of propane in the liquid-acid media, resulting in rather low currents and thereby precluding major commercial applications. To achieve high current density, it is necessary that propane readily accesses the anode catalyst, so it is necessary to use a gas-phase fuel cell.

The recent development of highly conducting polymers such as Nafion and improved cell designs have regenerated interest in low-temperature hydrocarbon fuel cells. In U.S. patent 6,294,068,[16] low-temperature polymer fuel cells based on Nafion were used for the partial oxidation of methane, ethane, and methanol, in either fuel cell or electrolysis mode, to form higher hydrocarbons. The authors also used PBI membranes for operation at higher temperatures (at least 200 °C). However, problems such as gas leakage and high internal resistance from the membrane electrode assembly (MEA) resulted in very low yields of hydrocarbon products.

Savadogo and Varela operated fuel cells at 95 °C and high humidification using Nafion and sulfuric-acid-doped PBI membranes as the electrolyte.[17] Both sulfuric-acid-doped PBI membranes and Nafion membranes needed high humidification to maintain ionic conductivity. The authors reported the formation of CO_2 and not propylene as the final product, but the mechanism was not discussed.

We will now show that propane reacts at the anode of H_3PO_4-doped PBI membrane fuel cells to form anode-catalyst-surface-bound hydrocarbon species that sequentially react further with water to form an oxygen-containing C_3 intermediate at the surface and then CO and CO_2 as the only volatile carbon-containing products.

Experimental Section

The fuel cell testing system was the same as that described in ref 5. The flow rates of the anode and cathode feeds were equal, typically 60 mL min^{-1} at atmospheric pressure. The inlet and effluent gas streams were analyzed using an on-line gas chromatograph (Hewlett-Packard Series II 5890), equipped with a packed-bed column and an integrator (Hewlett-Packard Series II 3396). Products were determined using a thermal conductivity detector (TCD) with helium as a carrier gas. Analyses were performed isothermally at 80 °C for 15 min. Propane (instrument grade 2.5; 99.5% purity, H_2O < 3 ppm, *n*-butane < 20 ppmw, methane < 300 ppmw, sulfur < 1 ppmw, ethane < 600 ppmw, isobutane < 3000 ppmw) was purchased from Praxair Canada.

PBI Membrane Preparation Procedure. The method of preparing PBI−H_3PO_4 membranes with 500−600 mol % acid loading was described previously.[5] In summary, high-MW (∼75,000) PBI powder (Aldrich) was dissolved in 9 times its weight of dimethylacetamide (DMAc, Aldrich) within 3 h at 150 °C in a closed Pyrex glass vessel. The solution so-obtained was then filtered to remove any residual particles and degassed at ambient temperature to eliminate the formation of air bubbles during casting, to reduce potential for defects in PBI films. Membrane films were prepared by warming solutions of high-MW PBI to dryness in an oven at 80 °C for 5 h. The resulting PBI film was immersed in distilled water until the membrane was self-supporting and could be detached readily from the glass surface. The PBI film then was heated at 195 °C for more than 12 h to eliminate residual traces of the DMAc solvent. The thickness of dry PBI membranes was in the range 87.5−100 μm, before doping with acid. The PBI membranes so-made were doped by immersion in 85 wt % aqueous H_3PO_4 solution (Aldrich). After the doping was completed, excess acid was removed from the PBI film surface using soft, dry tissue until a constant mass was obtained.

Preparation of Membrane Electrode Assemblies and the Cell Assembly. The catalyst powder, Pt/C (20 wt % Pt/Vulcan XC-72, Alfa Aesar) was dispersed as a suspension in a mixture of Nafion ionomer solution (5 wt % Aldrich) and ethanol having a weight ratio of 3:1:10. The suspension was applied separately by painting onto each face of the membrane, then dried using an infrared lamp. The platinum loading was 1 mg cm^{-2} for each electrode. The area of each electrode catalyst layer was close to 3.8 cm^2. Current collectors (metal mesh and carbon cloth) were situated across each surface, and the assembly was cold-pressed.

The resulting MEA was held between gas distribution plates fabricated from stainless steel SS316, a material having 18% chromium and 12% nickel.[18] SS316 is preferred over SS304, a commonly used stainless steel material, as it can better withstand corrosion. SS316 bipolar plates did not suffer corrosion during multiple successive tests each up to 24 h in duration. However, the same operation carried out using SS304 resulted in severe corrosion at the cell's surface.

The cell was connected to the load outside the test station by electrical wires connected to the outer surface of both plates. The inner surfaces of the plates were connected to the current collector. To provide a good seal, two thin Teflon gaskets were sized to accommodate both mesh and carbon cloth. The thickness of each gasket was made equal to the overall thickness of both mesh and carbon cloths.

Cell Operation and Determination of Performance. Anode and cathode inlet and outlet streams at anode and cathode compartments provided a continuous flow of reactants and tailing gases. The anode inlet stream was humidified by sparging the gas through deionized water in a closed in-line humidifier controlled at a temperature of 25 °C. The relative humidity in the cell was calculated from the water vapor pressure at the

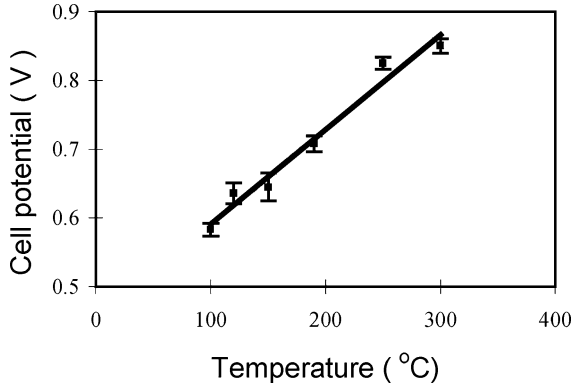

Figure 1. Variation of $C_3H_8-O_2$ fuel cells' open circuit potential with operating temperature at 1 atm after stabilization for at least 6 h.

humidification temperature compared to the saturated vapor pressure at the cell operating temperature. Humidification of the feed stream at 25 °C (P_{sat} 3.166 kPa) resulted in light humidification (relative humidity S_r 0.08%) in a fuel cell operated at 250 °C (P_{sat} 3977.6 kPa).

The cell was held in an oven equipped with a temperature controller to maintain the operation of the cell at specified temperatures.

The electrochemical performance of each cell was monitored using a Gamry electrochemistry instrument. The complex impedance of each cell was determined using electrochemical impedance spectroscopy, and the resistance (R) was determined from the Nyquist plot.

The results obtained for $C_3H_8-O_2$ fuel cells were each reproduced at least three times. Although the procedures were substantially the same for making all membranes, the R of the fuel cells varied between 0.2 and 0.4 Ω. A large R (1−2 Ω) indicated that the cell was not properly installed, so no further testing was performed in such cases.

Results and Discussion

Cell Potential. The open circuit potentials attained with $C_3H_8-O_2$ fuel cells at 1 atm were stable and reproducible. Cell potentials were obtained after stabilization at different temperatures for at least 6 h (Figure 1). The potentials increased with temperature, consistent with the Nernst equation. Thus, Pt anode catalysts deposited on PBI−H_3PO_4 readily chemisorbed and activated propane. The cell potential attained values over 0.8 V at temperatures higher than 200 °C, thus providing a significant driving force for electrochemical reactions.

Catalytic Dehydrogenation of Propane. The effectiveness of Pt/C (20 wt %)/PBI−H_3PO_4 as a dehydrogenation catalyst in the present system was tested by passing propane over the anode catalyst under anhydrous fuel cell operating conditions. The hydrogen concentration in the anode effluent increased with temperature, increasing rapidly over 250 °C. However, at temperatures lower than 200 °C, particularly 150 °C, no propylene was detected using gas chromatography analysis. Thus, any propylene formed was retained on the catalyst surface. Different catalyst loadings also affected the amount of hydrogen produced. Generally, the higher the platinum loading, the higher the concentration of H_2 in the effluent from the anode chamber. The concentration of hydrogen paralleled performance of the fuel cell when operated under anhydrous conditions. Clearly, cell performance improved as a result of the presence of catalytically generated H_2 that was then selectively oxidized in preference to propane.

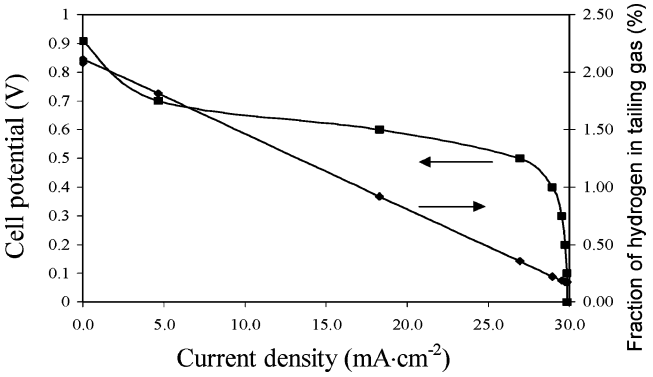

Figure 2. Polarization curve for H_2 (2 vol %) diluted with N_2 at 150 °C and the residual concentration of H_2 in the tailing gas. (R was 0.36 Ω.)

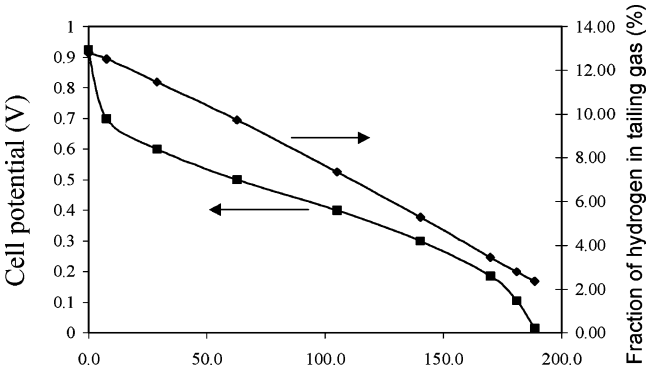

Figure 3. Polarization curve of H_2 (13 vol %) diluted with N_2 at 150 °C and the residual concentration of H_2 in tailing gas. (R was 0.36 Ω.)

Figures 2 and 3 show the effect of hydrogen partial pressure on the amount of electricity generated. Dilution with N_2 gas was used to emulate hydrocarbon fuel cell operation by simulating the H_2 partial pressure under selected conditions. Figure 2 shows a mass control region at current densities over 25.0 mA cm^{-2} for a stream containing 2% H_2. With propane, mass control was from access by propane to the catalyst, where hydrogen was generated by catalytic dehydrogenation of propane. Limited access by propane limited the amount of hydrogen present and thus limited the current density. Figure 3 shows the onset of a mass controlling region at higher current density, approximately 170 mA cm^{-2}, for a stream containing 13% H_2. These data are consistent with mass transport limitation. Propane transport to catalyst sites was limited in this region, thus catalytic generation of H_2 was also limited, resulting in reduction of the local partial pressure of H_2 as it was rapidly converted to protons at the anode−electrolyte interface. Explicitly, higher concentrations of H_2 resulted in higher current flow. It should be noted that not all H_2 was consumed during fuel cell operations. For the experiment shown in Figure 2, about 80% of H_2 (1.6% out of 2% present initially) was consumed at values before the mass transfer region. Approximately 90% of H_2 was consumed at maximum current density. Of the higher initial concentration of H_2 (Figure 3), 73% was consumed (3.5% of H_2 in tailing gas) at values before the mass transport region, and about 84% of hydrogen was consumed at maximum current density. There was a linear correlation between H_2 concentrations in the inlet stream and current flow (Figure 4). It was found that the equation derived from the correlation (shown in Figure 4) provided a reasonable match of the experimental values for current density using the present fuel cells to calculated values derived by assuming that the source of protons was a partial

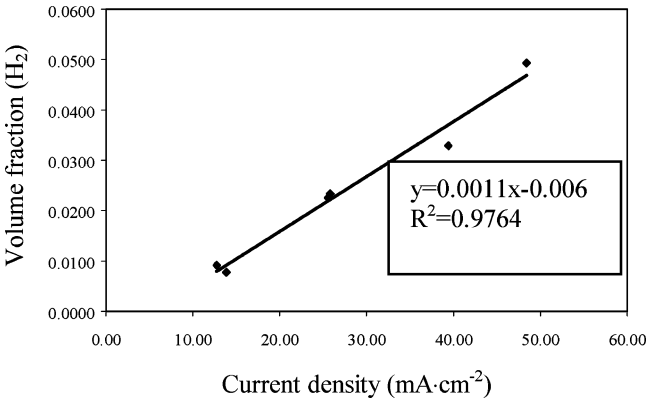

Figure 4. Correlation of H_2 concentration with current density at 150 °C under anhydrous conditions. (*R* was 0.38 Ω.)

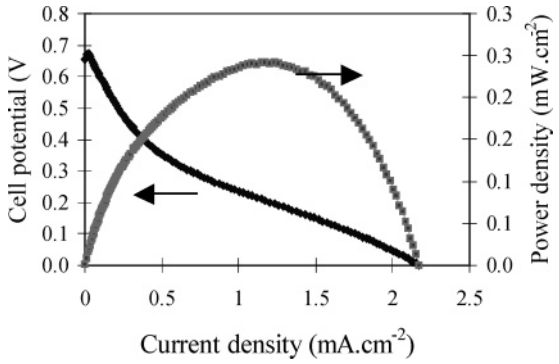

Figure 5. Polarization curve of $C_3H_8-O_2$ fuel cells under anhydrous conditions at 200 °C and 1 atm pressure. (*R* was 0.23 Ω.)

pressure of H_2 generated by the dehydrogenation of dry propane at catalyst sites.

Polarization Curves for Propane−Oxygen Fuel Cells: Anhydrous Conditions. The $C_3H_8-O_2$ fuel cells exhibited very low current flow during operation under anhydrous conditions (Figure 5). Further, even this low electrochemical activity rapidly diminished in the absence of humidity. Thus, not only was the current density low, the current flow was also not sustainable over an extended period of operation. After the cell had been working for 600 s at 0 mV, the current was reduced from the initial value of 2 mA cm^{-2} to about 0.3 mA cm^{-2}. This behavior is characteristic of the loss of catalyst activity due to the formation of deposits or strongly bound intermediate species on the catalyst surface, which then block access to active sites by further amounts of propane.

Polarization Curves for Propane−Oxygen Fuel Cells: Humid Conditions. Polarization curves for $C_3H_8-O_2$ fuel cells operated with humidification showed a significantly higher current flow (Figure 6). The addition of water had the effect of enabling the progress of electrochemical reactions, resulting in increased current flow, as was also found for $C_2H_6-O_2$ fuel cell systems (to be described in a forthcoming paper). When operated in potentiostatic mode, the initial current dropped during the initial few seconds, after which the current flow was sustainable, in contrast to operation under anhydrous conditions (Table 1). Current flow increased with decreased cell potential. Interestingly, when operation was carried out at low potential, 100 mV or short-circuit condition for an extended time (>10 min), the current flow increased gradually. This indicated that operation at low cell potential had the effect of "cleaning" the catalyst by reacting with strongly bound stable intermediate products, thus removing them from the catalyst's surface.

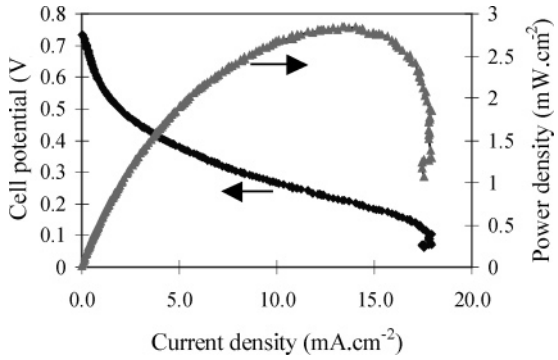

Figure 6. Polarization curve of $C_3H_8-O_2$ fuel cells at 250 °C and 1 atm pressure with light humidification (S_r 0.08%) of the anode feed. (*R* was 0.36 Ω.)

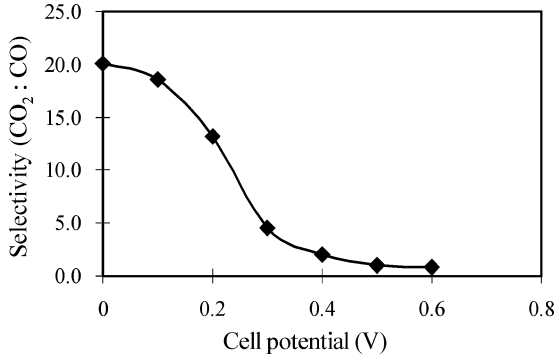

Figure 7. Dependence of the CO_2/CO ratio on the cell potential of $C_3H_8-O_2$ fuel cells operated at 250 °C and 1 atm pressure with light humidification (S_r 0.08%) of the anode feed.

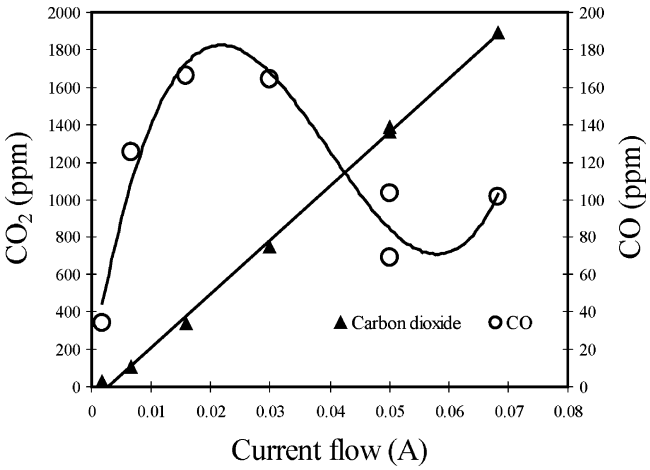

Figure 8. Variation of product concentrations with current flow for $C_3H_8-O_2$ fuel cells operated at 250 °C and 1 atm with light humidification (S_r 0.08%) of the anode feed.

While the mechanism of this process was not unequivocally definable from the present data, there was evidence available from the composition of the effluent. The apparent cleaning of the anode catalyst coincided with the decrease in CO in the effluent and concomitant increase in CO_2 at low potential (Figure 7) and higher current (Figure 8). At higher current, more water is produced at the cathode and is consumed at the anode, thus providing more oxygen for conversion of CO to CO_2. CO poisons Pt catalysts, especially at temperatures below 100 °C typical for operation of proton exchange membrane fuel cells (PEMFCs), as described on pp 89−90 and 152−155 of ref 4 and references therein. The proportion of Pt sites to which CO was strongly bound was lower in the present fuel cell at 250 °C than in PEMFCs operated at 100 °C. Nevertheless, those Pt

TABLE 1: Initial and Stable Current Flow for $C_3H_8-O_2$ Fuel Cells Operated at 250 °C and 1 atm with Light Humidification (S_r 0.08%) of the Anode Feed

	current density (mA cm^{-2})	
potential (mV)	initial value	after 1000 s
600	0.6	0.4
500	2.0	1.4
400	4.2	3.2
200	13.6	10.3
100	17.3	14.0

sites bound to CO were not active sites. Removal of CO from Pt by oxidizing it to CO_2 liberated those poisoned Pt sites and made them available to generate protons, thereby increasing current. In the present system, the oxidation process most probably was electro-oxidation in which the required oxygen atom originated from water at the anode.

The molar amounts of CO_2 and CO generated were quite similar throughout the high cell potential and low current flow region (Figure 7). In contrast, at cell potentials below 0.3 V, the amount of CO_2 became predominant, indicating that the electronic properties of the platinum catalyst differed with cell potential, thus influencing the activation of propane and further reactions of intermediate products. Easily desorbable products were formed at low potentials, so the rate of the formation of final products increased, and current flow also increased (Figure 8). The concentration of CO_2 in the effluent increased linearly with current, while that of CO reached a maximum value before declining at high currents.

Mechanism of Reactions in Propane Fuel Cells

Fuel cell operations carried out using propane as fuel under humid conditions produced CO_2 and CO as the only volatile products. This was consistent with the results obtained by Savadogo and Varela, who reported the formation of only CO_2 from direct propane fuel cells.[17] There was no crossover of O_2 from the cathode compartment to the anode compartment in our system, as shown by both gas chromatography monitoring and permeation testing. The membrane was proton-conducting, so neither O_2 nor oxide ions were the source of oxygen for the formation of CO and CO_2. Performance was stable under conditions of light humidification of the anode feed stream. Thus, water, which initially was introduced for the purpose of humidifying the membranes, was found to be a participant in the electrochemical reactions in the present acidic environment. Without water, the electrochemical reactions did not proceed readily or extensively.

The correlation between current density and amounts of CO and CO_2 formed showed that all hydrogen from propane was converted to protons and conducted via the membrane to the cathode, where water was formed. Water consumed at the anode was regenerated at the cathode.

Thus, the sources of the elemental compositions of the products are clear. However, the natures of the intermediates between propane and CO and CO_2 need to be identified. Two routes are feasible: (route 1) scission of C−C bonds followed by reaction with water to form oxides of carbon and (route 2) formation of oxygen-containing C_3 intermediates followed by C−C bond scission.

Route 1. It has been proposed that oxidation processes in acidic electrochemical cells involved the adsorption of saturated

SCHEME 1: Mechanism of Hydrocarbon Oxidation in Acidic Electrochemical Cells

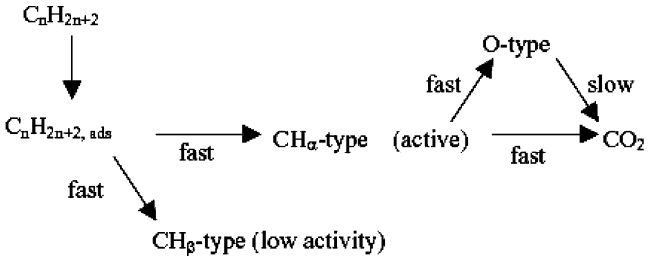

SCHEME 2: Proposed Intermediate Species Derived from Propane on a Platinum Surface[a]

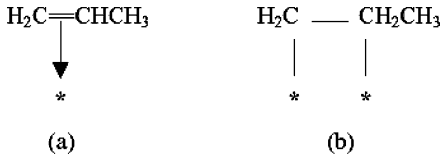

[a] The asterisk represents a surface site.

light hydrocarbons on the electrocatalyst followed by the rapid formation of oxidized intermediates, which are then slowly oxidized into CO_2.[19] Niedrach and Tochner showed that oxidation of paraffins C_nH_{2n+2} with $n \geq 2$ on platinum electrodes took place in two different potential regions and involved two distinct types of adsorbate species.[20] Brummer and Turner proposed that these adsorbates are O-type (oxygen-containing) and CH-type (Scheme 1),[21] the precise compositions of which are not known. The O-type is predominant in terms of coverage at all potentials, is the more highly oxidized species, and is the easiest to oxidize further to CO_2. Two CH-types, generalized as CH_α and CH_β, are less oxidized than the O-type, are harder to oxidize at higher potentials, and might include polymeric material. CH_α was found at all potentials and normally was less reactive toward oxidation than the O-type, whereas CH_β was less reactive toward either reduction or oxidation.

Niedrach proposed that, after the initial adsorption step, two significant reaction paths are available.[14] The more desirable path involves cracking to form a partially oxygen-containing intermediate, which is oxidized further to CO_2 at low potential. The second path results in the accumulation of relatively refractory multiple carbon species on the surface. Cairns and Breitenstein proposed that, after the initial adsorption step, the adsorbate is easily dehydrogenated further, resulting in formation of alkene-like intermediate species that then bond to multiple Pt catalyst sites, increasing C−C bond strain and leading to fracture of the molecules.[22] Bockris et al. proposed that the first step is the breaking of a C−H bond (eq 6).[23]

$$C_nH_{2n+2} \rightarrow C_nH_{2n+1,ads} + H_{ads} \quad (6)$$

The proposed second rate-determining step is a chemical surface reaction, which cracks the C−C bonds rather than the C−H bonds to produce hydrocarbon fragments on the surface of the noble metal catalysts.

$$C_nH_{2n+1\ ads} \rightarrow \text{slow} \rightarrow C_{1\ ads} + C_{2\ ads} \quad (7)$$

Scheme 2 shows the structures of possible intermediates on the platinum surface arising from dissociative adsorption. Partially dehydrogenated intermediate species formed at the platinum sites would not be expected to retain double bond

characteristics of π-bonded alkenes, because (a) adsorption of an alkene on a Pt surface typically involves two σ-bond interactions with adjacent Pt atoms and (b) results in the formation of a single C−C bond oriented parallel to the surface.[24]

In the above scheme, the formation of oxygen-containing species (Scheme 1) follows C−C bond scission (eq 7); however, the precise nature of the O-type intermediate is undefined. Thus, if the conversion of propane to carbon oxides involves the scission of C−C bonds before formation of oxygen-containing species, then the reaction sequence will be as shown in eqs 8−10 (where s indicates surface-bound species).

$$C_3H_8\,(g) \rightarrow C_3H_6\,(s) + 2H^+ + 2e^- \quad (8)$$

$$C_3H_6\,(s) + 3H_2O\,(g) \rightarrow 3C_1 \text{ species (s)} \rightarrow 3CO\,(g) + 12H^+ + 12e^- \quad (9)$$

$$3CO\,(g) + 3H_2O\,(g) \rightarrow 3CO_2\,(g) + 6H^+ + 6e^- \quad (10)$$

Route 2. The mechanism shown in Scheme 1 includes the production of surface species with low reactivity that would eventually result in deactivation of the anode catalyst. The present data indicate that all carbon from reacted propane forms either CO or CO_2. An alternative mechanism that accounts for this observation involves the reaction of water to form an oxygen-containing C_3 intermediate at the surface.

2-Propanol (IPA) is converted in fuel cells sequentially to acetone and then, via C−C bond scission steps, to CO and CO_2.[25−28] When a liquid fuel cell with a Nafion membrane was operated at 90 °C and IPA was dissolved in a greater amount of water, IPA was converted sequentially to acetone and CO_2.[25] Importantly, the performance of the IPA fuel cell was superior to that of a direct methanol fuel cell having a similar design and using the same materials. When, instead, a liquid fuel cell having a PBI−H_3PO_4 membrane was operated at 175 °C and IPA was in aqueous solution, the major product was again acetone.[26] Thus, a route to CO and CO_2 via an oxygen-containing C_3 intermediate is probably more facile than a route restricted to only capability to form a C_1 oxygen-containing intermediate surface species.

Hence, a very reasonable alternative mechanism for operation of the present propane fuel cell under light humidification conditions (eqs 11−14) differs from that under dry conditions. In the latter case, neither CO nor CO_2 was formed, only very small amounts of hydrocarbon species. The reaction under humid conditions was more extensive and produced only CO and CO_2. It is proposed that the surface-bound C_3 hydrocarbon species formed from propane reacted with either surface-bound water itself (eqs 11 and 13−16) or adjacent surface Pt−OH species derived from the reaction of water with Pt sites (eq 12)[29] to form oxygen-containing C_3 intermediates at the anode-catalyst surface, from which CO and CO_2 were subsequently derived (eq 13). Reaction with Pt−OH would have paralleled the sequence of reactions with water shown, regenerating Pt catalyst as shown in eq 15. It is well-established that Pt−OH species formed by reaction with water at the catalyst surface react with surface Pt−CO to form CO_2,[30−32] which then readily dissociates from the Pt surface and regenerates Pt sites. The resulting overall anode, cathode, and cell processes are summarized in eqs 16−18, respectively.

$$C_3H_8\,(g) \rightarrow C_3H_6\,(s) + 2H^+ + 2e^- \quad (11)$$

$$[Pt](s) + H_2O\,(g) \rightarrow [Pt]{-}OH\,(s) + H^+ + e^- \quad (12)$$

$$C_3H_6\,(s) + H_2O\,(g) \rightarrow \text{oxygen-containing } C_3 \text{ intermediate (s)}$$

$$\text{oxygen-containing } C_3 \text{ intermediate (s)} + 2H_2O \rightarrow \text{oxygen-containing } C_1 \text{ species (s)}$$

$$\text{oxygen-containing } C_1 \text{ species (s)} \rightarrow 3CO\,(g) + 12H^+ + 12e^- \quad (13)$$

$$3CO\,(g) + 3H_2O\,(g) \rightarrow 3CO_2\,(g) + 6H^+ + 6e^- \quad (14)$$

$$Pt{-}CO + Pt{-}OH \rightarrow 2Pt + CO_2 + H^+ + e^- \quad (15)$$

$$C_3H_8\,(g) + 6H_2O\,(g) \rightarrow 3CO_2\,(g) + 20H^+ + 20e^- \text{ (anode)} \quad (16)$$

$$5O_2\,(g) + 20H^+ + 20e^- \rightarrow 10H_2O\,(g) \text{ (cathode)} \quad (17)$$

$$C_3H_8\,(g) + 5O_2\,(g) \rightarrow 3CO_2\,(g) + 4H_2O\,(g) \text{ (net)} \quad (18)$$

Correlation of Data with Possible Mechanisms. Conclusions can be drawn from the combination of polarization curves and electrochemical products obtained. The low initial currents obtained under anhydrous conditions and their rapid deterioration showed the formation of catalyst-surface-bound species derived from propane and consequent blocking of catalyst-surface sites. It was probable that intermediate species as shown in Scheme 2b initially were formed by the dissociative chemisorption of propane. The detection of only CO and CO_2 as products showed that intermediates bonded strongly to the platinum-catalyst sites then reacted further at the surface and did not desorb as alkenes.[33] The effect of having intermediate species strongly bonded to the surface of platinum, which did not readily desorb, was that they had sufficient time to react further with water to form oxide species.

The environment at the PBI−H_3PO_4 membrane surface provided an acidic environment that enhanced C−C bond cleavage.[34] Less energy is required to break single C−C bonds than double bonds (C═C bond energy is 611 kJ mol^{-1}; C−C is 347 kJ mol^{-1}).[28] Further, the strength of a C−C single bond is reduced when a hydrocarbon is adsorbed onto a catalyst surface, compared to when it is in the gas phase.[35] Thus, C−C bonds would have been weakest when intermediate species bonded to multiple sites at the platinum surface, leading to the fragmentation to C_1 species. However, under dry conditions, the propane fuel cell produced very low current density, and even this poor performance was not sustainable. No detectable amount of methane, ethane, or ethylene was found in the anode effluent. These data suggest that the cracking mechanism (eqs 8 and 9) occurred to a very limited extent, at most.

The variation of product distribution with cell potential suggested that there were at least two electrochemical reaction pathways taking place,[36] but the nature of the reactions could not be fully discerned from the available data. Nonetheless, general insights were drawn. It appeared that, in the acidic environment, the anode electrochemical reactions resembled

steam reforming in that the components of H_2 (protons and electrons) and CO were formed, and this then reacted further to generate CO_2. The amounts of CO_2 and CO formed correlated well with the total current generated as protons were conducted through the electrolyte to the cathode.

No acetone was detected among the products from the present cell, in contrast to the above liquid fuel cell systems.[25−28] This is attributed to two factors; the present cell was operated at higher temperatures and was a gas-phase fuel cell.

The previous systems had aqueous liquid media in contact with the proton-conducting membrane. The high concentration of water at the interface with the catalyst would have promoted displacement of acetone from catalyst sites. Thus, the rate of C−C bond-breaking reactions to form C_1 species would be low, and hence the selectivity to CO and CO_2 was reduced. In the present system, the current density and the rate of formation of CO and CO_2 were both high under light humidification conditions, whereas there was a reduction in the formation of CO and CO_2 when an excess of water was present at high humidification.

Operation at temperatures as high as 250 °C afforded a higher rate of reaction than was attainable by the liquid fuel cell systems. In particular, the rate of the C−C bond scission steps would be higher, thus enhancing selectivity to C_1 products. The low water concentration in the lightly humidified feed stream was sufficient to enable reaction to form oxygen-containing intermediates. However, the water concentration was low, and the temperature was high, so C−C bond-breaking reactions of the oxygen-containing intermediate to form C_1 products predominated.

Thus, the combination of enhanced reaction rate at high temperature and the lack of displacement of the oxygen-containing C_3 intermediate by water resulted in the rapid formation of protons and CO and CO_2.

Consequently, the reaction sequence shown in eqs 11−18 is fully consistent with the electrochemical performance of the PBI fuel cell using propane as the hydrocarbon fuel and with the formation of CO and CO_2 as the only products from conversion of propane at the anode, via an oxygen-containing partial oxidation C_3 intermediate derived from reaction with H_2O.

Conclusions

Propane fuel cells using H_3PO_4-doped PBI polymer membranes produced low and unsustainable current densities at temperatures up to 250 °C under anhydrous conditions. Stable intermediate species blocked the surfaces of the noble metal catalysts, and the intermediate species could not react further into desorbable final products.

In contrast, when the anode feed stream was lightly humidified at 25 °C, sustainable and higher current densities were achieved. Water participated in the reaction sequence to generate an oxygen-containing partial oxidation C_3 intermediate and then CO and CO_2 as the only carbon-containing products.

Acknowledgment. This work was supported by the COURSE program of the Alberta Energy Research Institute, NOVA Chemicals, and the Natural Science and Engineering Research Council of Canada.

References and Notes

(1) Smith, J. M.; van Ness, H. C.; Abbott, M. M. *Introduction to Chemical Engineering Thermodynamics*, 5th ed.; McGraw-Hill International Editions: Singapore, 1996; p 638.
(2) Otsuka, T.; Ina, T.; Yamanaka, I. *Appl. Catal., A* **2003**, *247*, 219.
(3) Larminie, J.; Dicks, A. *Fuel Systems Explained*; Wiley: Chichester, U. K., 2000.
(4) Khordesch K.; Simader, G. *Fuel Cells and Their Applications*; VCH: New York, 1996.
(5) Cheng, C. K.; Luo, J. L.; Chuang, K. T.; Sanger, A. R. *J. Electrochim. Acta*, submitted for publication.
(6) Ledjeff-Hey, K.; Kalk, Th.; Mahlendorf, F.; Niemzig, O.; Trautmann, A.; Roes, J. *J. Power Sources* **2000**, *86*, 166.
(7) Hsu, M. S. U.S. Patent 5,747,185, 1998.
(8) Fischer, W. U.S. Patent 3,718,506, 1973.
(9) Mazanec, T. J.; Cable, T. L. U.S. Patent 4,933,054, 1990.
(10) Ahmed, S.; Kopasz, J.; Kumar R.; Krumplet, M. *J. Power Sources* **2002**, *112*, 519.
(11) Burwell, R. F.; Clausi, J. V.; Cohen, R.; Louie, C.; Watkins, D. S. U.S. Patent 5,360,679, 1994.
(12) Oswin, H. G.; Hartner, A. J.; Malaspina, F. *Nature* **1963**, *200*, 256.
(13) Cairns, E. J. *Nature* **1966**, *210*, 161.
(14) Niedrach, L. W. *J. Electrochem. Soc.* **1962**, *109*, 1092.
(15) Otsuka, K.; Yamanaka, I. *Catal. Today* **1998** *41*, 311.
(16) Petrovic, S.; Donini, J. C.; Thind, S. S.; Tong, S.; Sanger, A. R. U.S. Patent 6,294,068, 2001.
(17) Savadogo, O.; Varela, F. J. R. *J. New Mater. Electrochem. Syst.* **2000**, *4*, 93.
(18) Davies, D. P.; Adcock, P. L. Turpin, M.; Rowen, S. J. *J. Power Sources* **2000**, *86*, 237.
(19) Brummer, S. B.; Turner, M. J. *J. Phys. Chem.* **1967**, *71*, 3902.
(20) Niedrach, L. W.; Tochner, M. *J. Electrochem. Soc.* **1967**, *114*, 17.
(21) Brummer, S. B.; Turner, M. J. *J. Phys. Chem.* **1967**, *71*, 2825.
(22) Cairns, E. J.; Breitenstein, A. M. *J. Electrochem. Soc.* **1967**, *114*, 764.
(23) Bockris, J. O. M.; Gileadi, E.; Stoner, G. E. *J. Phys. Chem.* **1969**, *73*, 427.
(24) Zarea, F. *Prog. Surf. Sci.* **2001**, *69*, 1.
(25) Cao, D.; Bergens, S. H. *J. Power Sources* **2003**, *124*, 12.
(26) Wang, J. T.; Wasmus, S.; Savinell, R. F. *J. Electrochem. Soc.* **1995**, *142*, 4218.
(27) Qi, Z. G.; Hollett, M.; Attia, A.; Kaufman, A. *Electrochem. Solid-State Lett.* **2002**, *5*, A 129.
(28) Qi, Z. G.; Kaufman, A. *J. Power Sources* **2002**, *112*, 121.
(29) Gokagac, G.; Kennedy, B. J. *Z. Naturforsch., B: Chem. Sci.* **2002**, *57*, 193.
(30) Carette, L.; Friedrich, K. S.; Stimming, U. *Fuel Cells* **2001**, *1*, 5.
(31) Mukerjee, S.; Lee, S. J.; Ticianelli, E. A.; McBreen, J.; Grgur, B. N.; Markovic, N. M.; Ross, P. N.; Giallombardo, J. R.; De Castro, E. S. *Electrochem. Solid-State Lett.* **1999**, *2*, 12.
(32) Baschuk, J. J., Li, X. *Int. J. Energy Res.* **2001**, *25*, 695.
(33) Kemball, C.; Taylor, H. S. *J. Am. Chem. Soc.* **1948**, *70*, 345.
(34) Uzio, D.; Didillon, B.; Pellier, E. U.S. Patent 6,498,280, 2002.
(35) Wade, L. G., Jr. Alkenes: Structure and Synthesis. In *Organic Chemistry*; Prentice-Hall: Englewood Cliffs, NJ, 1987, p 241.
(36) Fahmi, A.; van Santen, R. A. *J. Phys. Chem.* **1996**, *100*, 5676.